MULTI-FIELD STABILIZED FINITE ELEMENT APPROXIMATIONS FOR NONLINEAR VISCOPLASTICITY USING THE SMD FLUID MODEL

Daniel Dall'Onder dos Santos, dallonder@mecanica.ufrgs.br
Sérgio Frey[1], frey@mecanica.ufrgs.br
Laboratory of Computational and Applied Fluid Mechanics (LAMAC) - Mechanical Engineering Department- Federal University of Rio Grande do Sul - Rua Sarmento Leite, 425 - 90050-170 – Porto Alegre, RS, Brazil

Abstract. *This work concerned with a numerical study of non-linear viscoplastic materials subjected to inertia flows. The mechanical model employed the continuity and motion equations coupled with a rheological model for non-linear viscoplasticity, recently introduced by Souza Mendes and Dutra (2004) – the so-called SMD fluid model. Numerical approximations for the governing equations have been carried out via a multi-field stabilized finite element method - based on the Galerkin least-squares methodology - which has as primal variables extra-stress, pressure and velocity fields. Aiming to investigate the morphology of yield surfaces of viscoplastic materials flowing under inertia influence, some two-dimensional numerical simulations of inertia flows of an SMD fluid around the confined cylinder have been performed. The aspect ratio between the channel and the cylinder has been fixed as two-to-one, and the rheological and kinematic properties of SMD fluid flows have been considered as follows: the SMD dimensionless viscoplastic number – the jump number – was ranged from 1 to 100, the power-law index from 0.5 to 1.0, the dimensionless flow-rate from 0.25 to 1.0 and the Reynolds number from 4 to 29. In all computations, the primal variables have been approximated by equal-order Lagrangian bi-linear interpolations – violating, in this way, the compatibility conditions involving the extra stress-velocity and pressure-velocity finite element sub-spaces. The obtained results have confirmed the good stability features of the multi-field formulation and were physically meaningful.*

Keywords: Viscoplastic fluids, SMD model, Multi-field stabilized formulation, Galerkin least-squares methodology, flow around a confined cylinder.

1. INTRODUCTION

Although viscoplastic fluid models do not describe normal stress differences or time-dependent elastic effects, they have been used to predict the mechanical behavior of a large class of industrial materials. These models may describe an yield stress limit for the material, *i. e.*, it only flows when the applied stress lies beyond this limit. Among classical constitutive equations employed to model viscoplasticity, Bingham, Herschel-Bulkley and Casson models may be quoted (Bird *et al.*, 1987).

However, in the last decade, experimental observations of viscoplastic materials (Barnes, 1999) have lead to the conclusion that the yield stress actually is an apparent phenomenon and it could only be employed to model the mechanical behavior of some structured liquids. This class of non-Newtonian fluids present severe changes in their mechanical properties within a very small range of stress - as pointed out, for instance, by Souza Mendes and Dutra (2004). In this article, the authors introduced a new constitutive model for non-linear viscoplastic materials, which has proved to be able to prescribe a complete flow curve for viscoplastic materials. First, for low stress ranges, the material presents a high Newtonian viscosity; second, for a stress range around its apparent yield limit, the material suffers drastic changes in its structure, presenting a jump in the shear rate; and last, for stresses higher than the yield stress, the fluid shear-thins – see, for a detailed explanation, Souza Mendes and Dutra (2004).

The main goal of this article has been to perform two-dimensional finite element approximations for a non-linear viscoplastic materials flowing under inertia influence. Hence, it has employed the viscoplastic equation introduced by Souza Mendes and Dutra (2004) – hereafter, simply called SMD fluid. This model has been approximated via a multi-field stabilized method for extra-stress, pressure and velocity, based on Galerkin least-squares strategy. This methodology, introduced by Hughes *et al.* (1986) for the Stokes problem and later extended to incompressible Navier-Stokes equations in Franca and Frey (1992), does not need to satisfy the compatibility conditions arisen from finite element sub-spaces for extra-stress-velocity and velocity-pressure fields. In addition, it enhances the classical Galerkin stability by adding mesh-dependent terms which are functions of the residuals of Euler-Lagrange equations, evaluated element-wise. Since these residuals are trivially satisfied by the exact solution of the problem, consistency is preserved in these class of method.

In this article, SMD fluid flows around a circular cylinder inside a planar channel, with a fixed aspect ratio of two-to-one, have been numerically simulated. In order to evaluate the influence of yield stress limit, shear-thinning, flow-rate and inertia on yield surfaces of viscoplastic materials, the SMD dimensionless number – the jump number, *J* – has been ranged from 1 up to 100, the power-law index from 0.5 to 1.0, the dimensionless flow-rate, *u**, from 0.25 to 1.0

---

[1] Corresponding author.

and the Reynolds number form 4 to 29, respectively. In numerical simulations, a combination of equal-order Lagrangian bilinear interpolations have been employed to approximate the primal variables of the problem, violating the compatibility conditions involving the finite element sub-spaces for these variables. Numerical results generated in this work have reassured the fine stability features of the employed multi-field stabilized formulation and have been able to describe the flow dynamics of non-linear viscoplastic materials.

2. THE MECHANICAL MODEL

From the principles of mass conservation and momentum balance (Astarita and Marrucci, 1974), the following multi-field formulation for flows of inelastic non-Newtonian fluids may be stated ,

$$
\begin{aligned}
&\rho([\nabla \mathbf{u}]\mathbf{u}) - \operatorname{div} \boldsymbol{\tau} + \nabla p = \mathbf{f} && \text{in } \Omega \\
&\boldsymbol{\tau} - 2\eta(\dot{\gamma})\mathbf{D}(\mathbf{u}) = 0 && \text{in } \Omega \\
&\operatorname{div} \mathbf{u} = 0 && \text{in } \Omega
\end{aligned}
\tag{1}
$$

where Ω is the flow domain, $\mathbf{u}$ the fluid velocity, ρ the density, $\boldsymbol{\tau}$ the extra-stress tensor, p the hydrostatic pressure and $\mathbf{f}$ the body force vector.

For inelastic non-Newtonian fluids, the extra-stress tensor may be modeled as a generalized Newtonian liquid (GNL) (Bird *et al.*, 1987),

$$
\boldsymbol{\tau} = 2\eta(\dot{\gamma})\mathbf{D}
\tag{2}
$$

where $\eta(\dot{\gamma})$ is the apparent fluid viscosity, a function of the second invariant of the strain rate tensor, $\mathbf{D}$ (Bird *et al.*, 1987),

$$
\dot{\gamma} = (2\operatorname{tr}\mathbf{D}^2)^{1/2}
\tag{3}
$$

The apparent viscosity function used in this work was the one recently introduced by Souza Mendes and Dutra (2004) for non-linear viscoplastic materials. This new material equation, thereafter just referred as SMD, has been already proved suitable for a wide class of real viscoplastic liquids. The SMD model for shear stress may be expressed by the following expression,

$$
\tau = (1 - \exp(-\eta_0 \dot{\gamma}/\tau_0))(\tau_0 + K\dot{\gamma}^n)
\tag{4}
$$

where τ_0 is the yield stress of the viscoplastic material, K its consistency index, η_0 its Newtonian viscosity for very low values of shear rate n the power-law exponent, which controls the viscosity shear-thinning beyond the material yield limit, and τ the magnitude of the shear stress tensor, $\boldsymbol{\tau}$, given by

$$
\tau = (1/2\operatorname{tr}\boldsymbol{\tau}^2)^{1/2}
\tag{5}
$$

From Eq. (2) and (4), the SMD viscosity function may be written as

$$
\eta(\dot{\gamma}) = (1 - \exp(-\eta_0 \dot{\gamma}/\tau_0))(\frac{\tau_0}{\dot{\gamma}} + K\dot{\gamma}^{n-1})
\tag{6}
$$

with the magnitude of the shear rate tensor $\mathbf{D}$ given by Eq. (3).

3. FINITE ELEMENT MODELING

Assuming a bounded flow domain $\Omega \subset \Re^2$, with a regular boundary Γ. Based on the multi-field formulation defined by Eq. (1) coupled with the SMD viscosity function, Eq. (6), a multi-field boundary-value problem for inertia flows of nonlinear viscoplastic fluids may be stated as,

$$
\begin{aligned}
&\rho([\nabla\mathbf{u}]\mathbf{u})-\operatorname{div}\boldsymbol{\tau}+\nabla p=\mathbf{f} && \text{in } \Omega\\
&\boldsymbol{\tau}-2(1-\exp(-\eta_0(2\operatorname{tr}\mathbf{D}^2)^{1/2}/\tau_0))(\tau_0(2\operatorname{tr}\mathbf{D}^2)^{-1/2}+K(2\operatorname{tr}\mathbf{D}^2)^{(n-1)/2})\mathbf{D}(\mathbf{u})=0 && \text{in } \Omega\\
&\operatorname{div}\mathbf{u}=0 && \text{in } \Omega\\
&\mathbf{u}=\mathbf{u}_g && \text{on } \Gamma_g\\
&[-p\,\mathbf{I}+\boldsymbol{\tau}]\mathbf{n}=\mathbf{t}_h && \text{on } \Gamma_h
\end{aligned}
\tag{7}
$$

where $\mathbf{I}$ is the unity tensor, $\mathbf{n}$ the outward unit vector, $\mathbf{t}_h$ the stress vector, Γ_g and Γ_h the portions of boundary Γ on which Dirichlet and Neumann conditions are imposed, respectively, and the remaining variables and parameters defined as previously.

The finite element approximation for the multi-field boundary-problem defined by Eq. (7) may be built employing the following finite element sub-spaces for extra stress ($\boldsymbol{\Sigma}^h$), velocity ($\mathbf{V}^h$) and pressure (P^h) fields,

$$
\begin{aligned}
&\mathbf{V}^h=\{\mathbf{v}\in H_0^1(\Omega)^N|\mathbf{v}_{|K}\in R_k(K)^N,\ K\in\Omega^h\}\\
&\mathbf{V}_g^h=\{\mathbf{v}\in H^1(\Omega)^N|\mathbf{v}_{|K}\in R_k(K)^N,\ K\in\Omega^h,\ \mathbf{v}=\mathbf{u}_g\text{ on }\Gamma_g\}\\
&P^h=\{p\in C^0(\Omega)\cap L_2^0(\Omega)|p_{|K}\in R_l(K),\ K\in\Omega^h\}\\
&\boldsymbol{\Sigma}^h=\{\mathbf{S}\in C^0(\Omega)^{NxN}\cap L_2(\Omega)^{NxN}|S_{ij}=S_{ji},i,j=1,N,\ \mathbf{S}_{|K}\in R_m(K)^{NxN},\ K\in\Omega^h\}
\end{aligned}
\tag{8}
$$

with R_k, R_l and R_m denoting polynomial spaces of degree k, l and m, respectively, the functional space of continuous functions $C^0(\Omega)$ and the Sobolev space $H^1(\Omega)$ defined in the usual way (Ciarlet, 1978) and the Hilbert and Sobolev space $L_2^0(\Omega)$ and $H_0^1(\Omega)$ defined, respectively, by

$$
\begin{aligned}
&L_2^0(\Omega)=\{q\in L_2(\Omega)\,|\,\int_\Omega q\,d\Omega=0\}\\
&H_0^1(\Omega)=\{w\in H^1(\Omega)\,|\,\partial_{x_i}w\in L^2(\Omega)\,|\,w=0\ \ on\,\Gamma_g,\ i=1,N\}
\end{aligned}
\tag{9}
$$

3.1 A multi-field stabilized formulation

Based on the finite element sub-spaces defined by Eq. (8), a multi-field stabilized Galerkin least-squares-like formulation for SMD viscoplastic fluid flows may be written as: *given the functions of body force* $\mathbf{f}$ *and Dirichlet and Neumann boundary conditions* $\mathbf{t}_h$, *and* $\mathbf{u}_g$, *respectively, find the triple* $(\boldsymbol{\tau}^h,p^h,\mathbf{u}^h)\in\boldsymbol{\Sigma}^h\times P^h\times\mathbf{V}_g^h$ *such that*

$$
B(\boldsymbol{\tau}^h,p^h,\mathbf{u}^h;\mathbf{S}^h,q^h,\mathbf{v}^h)=F(\mathbf{S}^h,q^h,\mathbf{v}^h)\quad\forall\,(\mathbf{S}^h,q^h,\mathbf{v}^h)\in\boldsymbol{\Sigma}^h\times P^h\times\mathbf{V}_g^h
\tag{10}
$$

with

$$
\begin{aligned}
B(\boldsymbol{\tau}^h,p^h,\mathbf{u}^h;&\mathbf{S}^h,q^h,\mathbf{v}^h)=[2(1-\exp(-\eta_0(2\operatorname{tr}\mathbf{D}^2)^{1/2}/\tau_0))(\tau_0(2\operatorname{tr}\mathbf{D}^2)^{1/2}+K(2\operatorname{tr}\mathbf{D}^2)^{(n-1)/2})]^{-1}\int_\Omega\boldsymbol{\tau}^h\cdot\mathbf{S}^h d\Omega\\
&+\int_\Omega\rho([\nabla\mathbf{u}^h]\mathbf{u}^h)\cdot\mathbf{v}^h d\Omega-\int_\Omega\boldsymbol{\tau}\cdot\mathbf{D}(\mathbf{v}^h)d\Omega-\int_\Omega p\operatorname{div}\mathbf{v}^h d\Omega+\int_\Omega\operatorname{div}\mathbf{u}^h q^h d\Omega+\epsilon\int_\Omega p^h q^h d\Omega-\int_\Omega\mathbf{D}(\mathbf{u})^h\cdot\mathbf{S}^h d\Omega\\
&+\sum_{K\in\Omega^h}\int_{\Omega_K}(\rho[\nabla\mathbf{u}^h]\mathbf{u}^h+\nabla p^h-\operatorname{div}\boldsymbol{\tau})\cdot(\alpha(\operatorname{Re}_K)(\rho[\nabla\mathbf{v}^h]\mathbf{u}^h+\nabla q^h-\operatorname{div}\mathbf{S}^h))d\Omega+\delta\int_\Omega\operatorname{div}\mathbf{u}^h\operatorname{div}\mathbf{v}^h d\Omega\\
&+2(1-\exp(-\eta_0(2\operatorname{tr}\mathbf{D}^2)^{1/2}/\tau_0))(\tau_0(2\operatorname{tr}\mathbf{D}^2)^{1/2}+K(2\operatorname{tr}\mathbf{D}^2)^{(n-1)/2})\beta\,.\\
&\qquad\qquad\cdot\int_\Omega([2(1-\exp(-\eta_0(2\operatorname{tr}\mathbf{D}^2)^{1/2}/\tau_0))(\tau_0(2\operatorname{tr}\mathbf{D}^2)^{-1/2}+K(2\operatorname{tr}\mathbf{D}^2)^{(n-1)/2})]^{-1}\boldsymbol{\tau}^h-\mathbf{D}(\mathbf{u})^h).\\
&\qquad\qquad\quad\cdot([2(1-\exp(-\eta_0(2\operatorname{tr}\mathbf{D}^2)^{1/2}/\tau_0))(\tau_0(2\operatorname{tr}\mathbf{D}^2)^{-1/2}(2\operatorname{tr}\mathbf{D}^2)^{(n-1)/2})]^{-1}\mathbf{S}^h-\mathbf{D}(\mathbf{v})^h)d\Omega
\end{aligned}
\tag{11}
$$

and

$$
F(\mathbf{S}^h,q^h,\mathbf{v}^h)=\int_\Omega\mathbf{f}\cdot\mathbf{v}^h d\Omega+\int_{\Gamma_h}\mathbf{t}_h\cdot\mathbf{v}^h d\Gamma+\sum_{K\in\Omega^h}\int_{\Omega_K}\mathbf{f}\cdot(\alpha(\operatorname{Re}_K)(\rho[\nabla\mathbf{v}^h]\mathbf{u}^h+\nabla q^h-\operatorname{div}\mathbf{S}))d\Omega
\tag{12}
$$

where the grid Reynolds number Re_K *and the stability parameters* $\alpha(Re_K)$ *and* δ *are defined as in Franca and Frey (1992),*

$$\alpha(\mathrm{Re}_K) = \frac{h_K}{2|\boldsymbol{u}^h|_p} \xi(\mathrm{Re}_K)$$

$$\xi(\mathrm{Re}_K) = \begin{Bmatrix} \mathrm{Re}_K, & 0 < Re_K < 1 \\ 1, & \mathrm{Re}_K > 1 \end{Bmatrix}$$

$$\mathrm{Re}_K = \frac{\rho\, h_K |\boldsymbol{u}^h|_p\, m_k}{4(1-\exp(-\eta_0(2\mathrm{tr}\,\mathbf{D}^2)^{1/2}/\tau_0))(\tau_0(2\mathrm{tr}\,\mathbf{D}^2)^{-1/2}+K\,\dot{\gamma}^{n-1})} \qquad (13)$$

$$m_k = \min\{1/3, 2\,C_k\}$$

$$C_k \sum_{K \in \Omega^h} h_K^2 \|\mathrm{div}\,\mathbf{S}^h\|_{0,K}^2 \geq \|\mathbf{S}^h\|_K^2 \quad \forall\, \mathbf{S}^h \in \boldsymbol{\Sigma}^h$$

the stabilized parameter of the SMD viscoplastic constitutive equation, β, set as 0.25, according the error estimate introduced in Behr et al. (1993).

3.2 Nonlinear strategy

The substitution of finite element approximations for the trial functions ($\boldsymbol{\tau}^h, p^h, \mathbf{u}^h$) and their respective test functions ($\mathbf{S}^h, q^h, \mathbf{v}^h$) - expressed as linear combinations of shape functions and unknown degrees of freedom – in the stabilized formulation defined by Eq. (10)-(13), gives rise to the following set of residual equations,

$$\mathbf{R}(\mathbf{U}^h) = \mathbf{0} \qquad (14)$$

where **U** is the vector of degrees of freedom formed by $\boldsymbol{\tau}$, **p** and **u** at all nodal points, $\mathbf{U} = [\boldsymbol{\tau}, \mathbf{p}, \mathbf{u}]^T$, and **R(U)** is given by the set of matrices

$$\mathbf{R}(\mathbf{U}) = [(1+\beta)\mathbf{E}(\eta(\dot{\gamma})) + (1-\beta)\mathbf{H} + \mathbf{E}_\alpha(\mathbf{u})]\boldsymbol{\tau} + [\mathbf{N}(\mathbf{u}) + \mathbf{N}_\alpha(\mathbf{u}) - \beta\mathbf{K} - (1+\beta)\mathbf{H}^T - \mathbf{G}^T + \boldsymbol{\delta}]\mathbf{u}$$
$$+ [\mathbf{G} + \mathbf{G}_{\boldsymbol{\alpha}}(\mathbf{u}) + \boldsymbol{\epsilon}]\mathbf{p} - [\mathbf{F} + \mathbf{F}_{\boldsymbol{\alpha}}(\mathbf{u})] \qquad (15)$$

where [**H**] is the matrix derived from the surface force term of motion equation, and [$\mathbf{H}^T$] the matrix from the stress-deformation relation term of SMD viscoplastic equation, [**E**] the matrix from extra-stress term of SMD viscoplastic equation, [**N**] the matrix from the inertia force term of motion equation, [**K**] the matrix from the diffusive term of SMD viscoplastic equation, [**G**] and [$\mathbf{G}^T$] the matrices from the pressure term of motion equation and incompressibility term of continuity equation, respectively, and [**F**] the matrix from the body force-term of motion equation. Matrices with α-subscript are derived from the stabilized terms of motion equation, [$\boldsymbol{\delta}$] the matrix from δ-stabilized-term of continuity equation and [$\boldsymbol{\varepsilon}$] the matrix from the ε-term of continuity equation.

In order to solve the residual set of non-linear equation defined by Eq. (14)-(15), the following quasi-Newton algorithm may be introduced,

Algorithm:

I. Estimate the vector $\mathbf{U}_{k=0}$ and set the convergence criterion ε as 10^{-7}.
II. Solve for the incremental vector $\mathbf{a}_{k+1}$ the linear system,

$$\mathbf{J}(\mathbf{U}_k)\mathbf{a}_{k+1} = -\mathbf{R}(\mathbf{U}_k) \qquad (16)$$

where **R(U)** is given by Eq. (15) and the Jacobian matrix **J(U)** defined by

$$\mathbf{J}(\mathbf{U}) = (1+\beta)\mathbf{E}(\eta(\dot{\gamma})) + (1-\beta)\mathbf{H} + \mathbf{E}_\alpha(\mathbf{u}, \eta(\dot{\gamma})) + [\partial_{\mathbf{U}}(\mathbf{E}_\alpha(\mathbf{u}, \eta(\dot{\gamma})))]\boldsymbol{\tau}$$
$$+ \mathbf{M} + \mathbf{N}(\mathbf{u}) + \mathbf{N}_\alpha(\mathbf{u}, \eta(\dot{\gamma})) + \beta\mathbf{K} - (1+\beta)\mathbf{H}^T - \mathbf{G}^T + [\partial_{\mathbf{U}}(\mathbf{N}(\mathbf{u}) + \mathbf{N}_\alpha(\mathbf{u}, \eta(\dot{\gamma})))]\mathbf{u} \qquad (17)$$
$$+ \mathbf{G} + \mathbf{G}_\alpha(\mathbf{u}, \eta(\dot{\gamma})) + \mathbf{P} + [\partial_{\mathbf{U}}(\mathbf{G}_\alpha(\mathbf{u}, \eta(\dot{\gamma})))]\mathbf{p} + \partial_{\mathbf{U}}(\mathbf{F}_\alpha(\mathbf{u}, \eta(\dot{\gamma})))$$

III. Compute the vector $\mathbf{U}_{k+1}$:

$$\mathbf{U}_{k+1} = \mathbf{U}_k + \mathbf{a}_{k+1} \qquad (18)$$

IV. If $|\mathbf{R}(\mathbf{U}_{k+1})|_{\infty} > \epsilon$, then update k and go back to step II; otherwise, store solution $\mathbf{U}_{k+1}$ and exit the algorithm.

Remark: As initial solution estimative, null velocity, pressure and extra stress fields have been employed.

4. NUMERICAL RESULTS

In this section, a multi-field stabilized formulation, defined by Eq. (10)-(13), has been employed to approximate SMD fluid flows around a cylinder of circular cross-section kept inside a planar channel. Due to the geometric symmetry of the problem, only one half of the domain has been considered in all computations. The imposed velocity and extra-stress boundary conditions were: uniform parallel velocity u_0 at channel inlet and outlet, no-slip and impermeability on channel walls and cylinder surface, and symmetry conditions at channel centerline ($\partial_2 u_1 = u_2 = \tau_{12} = 0$). The channel aspect ratio, namely the half channel width (H) divided by the cylinder radius (R), has been set as two-to-one. In order to guarantee fully-developed flows upstream and downstream of the cylinder, the mesh length either before or after the cylinder has been equal to $17R$ – see Fig. 1a for the problem statement.
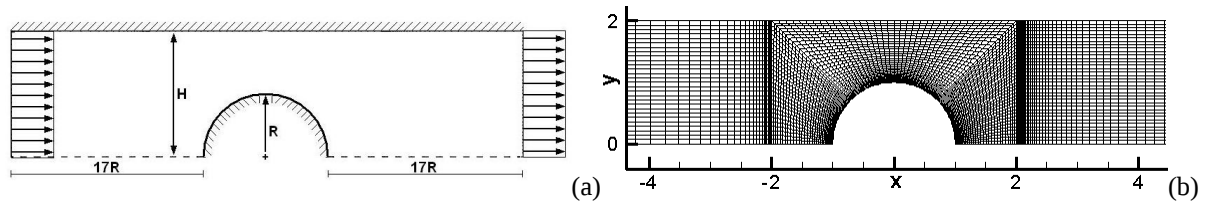

Figure 1. Flow around a cylinder: (a) problem statement; (b) detail of the employed mesh around the cylinder.

In order to investigate the flow dynamics of SMD fluids, Souza Mendes *et. al* (2007) introduced a new viscoplastic dimensionless parameter – so-called jump number, J -which takes into account the relative measure of shear rate jump when the shear stress is approximately equal to the material stress limit, τ_0. (This may be seen at the dimensionless SMD flowchart and viscosity curve shown in Fig. 2). Mathematically, the jump number may be given by

$$J \equiv \frac{\dot{\gamma}_1 - \dot{\gamma}_0}{\dot{\gamma}_0} = \frac{\eta_0 \tau_0^{(1-n)/n}}{K^{1/n}} \tag{19}$$

since $\dot{\gamma}_0$ and $\dot{\gamma}_1$ are, respectively, the shear rate values at the beginning of the shear rate jump and at the power-law region, *i. e.*, $\dot{\gamma}_0 \equiv \tau_0/\eta_0$ and $\dot{\gamma}_1 \equiv (\tau_0/K)^{1/n}$ - see Souza Mendes *et. al* (2007) for more details..
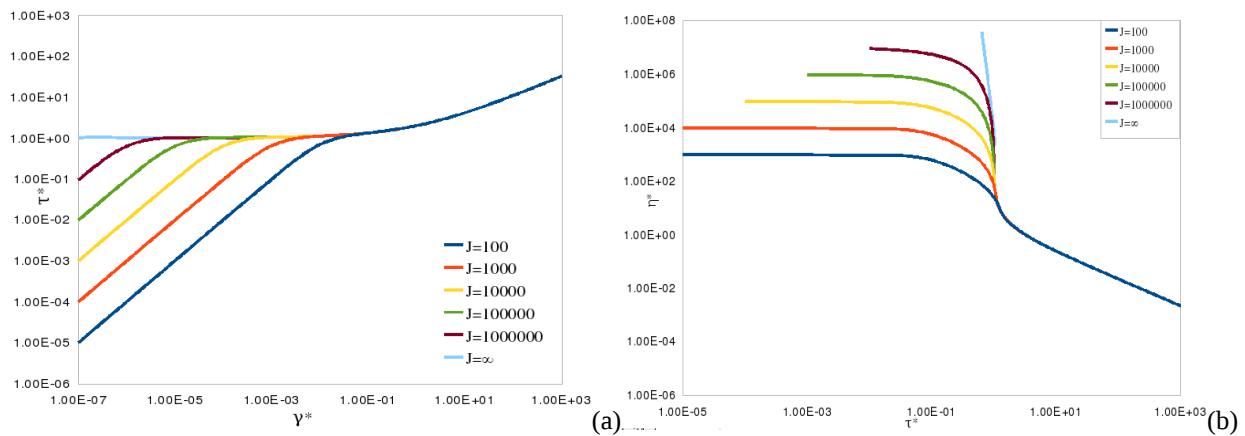

Figure 2. Dimensionless SMD model for n=0.5: (a) Flow chart; (b) SMD viscosity function.

In addition, to study the influence of inertia effects on viscoplastic fluid flows, the Reynolds number based on the power-law viscosity function has been stated as

$$\mathrm{Re} = \frac{\rho u_c^{(2-n)} L_c^n}{K} \tag{20}$$

where the characteristic velocity u_c was the velocity at the channel inlet and the characteristic length L_c was the half channel width (*H*); the remaining variables have been defined as previously.

In the numerical simulations, the jump number, *J*, was investigated from 1 to 100, the power law index, *n*, from 0.5 to 1.0, the Reynolds number from 4 to 29 and the dimensionless average velocity in the inlet channel, $u^* = (u K^{1/n})/(\tau_0^{1/n} L_c)$, from 0.25 to 1.0. After a mesh independence procedure, it has been chosen a finite element mesh consisting of a combination of equal order bi-linear Lagrangian elements ($Q_1/Q_1/Q_1$), for extra-stress, velocity and pressure. The total number of elements was 11,584 and the number of nodal points was 11,957, and the mesh was more refined at the vicinity of the cylinder – see Fig. 1b for a detail of the selected mesh.

The influence of the jump number on the development of unyielded zones (the black ones in the figures) in SMD viscoplastic inertialess fluid flows has been shown in Fig. 3. In this figure, the jump number was varied from *J*=1 (Fig. 3a and 3c) to *J*=100 (Fig. 3b and 3d), the Reynolds number was set as zero, the power law index as 1.0 and the dimensionless inlet velocity – the flow rate – as 1.0. One may observe that, as *J* grows, the size of unyielded regions at the cylinder vicinity was strongly reduced - regions subjected to high strain rates. On the other hand, the regions of fully developed flow upstream and downstream of the cylinder – the so-called plug flows – were only lightly influenced by the growth of jump number, since those regions correspond to very low strain rates. The pressure drop has also experimented a low increasing as the jump number *J* increased – compare Fig. 3c, for *J*=1, and Fig. 3d, for *J*=100. Besides, from the numerical point of view, the smooth pressure contours illustrated in Fig. 3d – for *J*=100, assured the good stability features of the employed multi-field method even for flows subjected to a very high material non-linearity
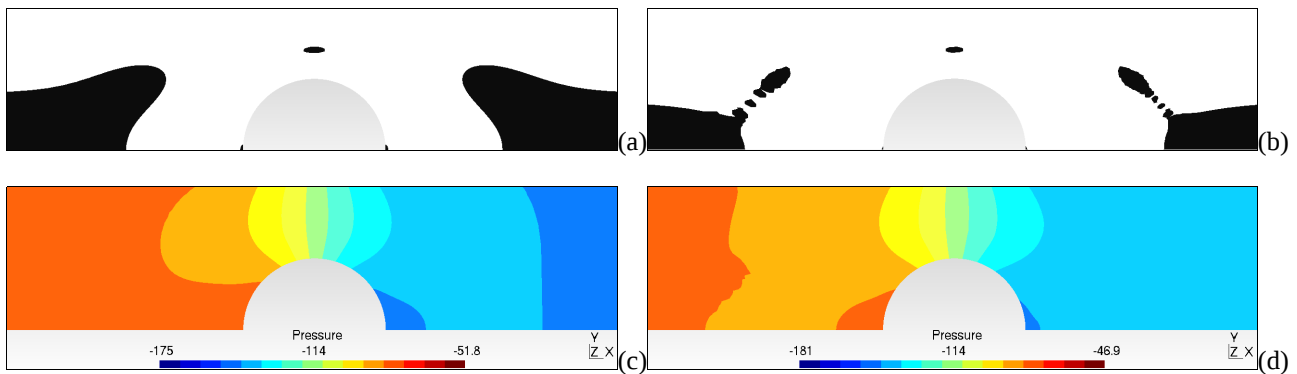

Figure 3. Yield surfaces and pressure contours, for Re=0, *n*=1.0 and *u**=1.0: (a) and (c) *J*=1; (b) and (d) *J*=100.

In Fig. 4, the yielded (the white ones in the figures) and unyielded zones, still for inertialess flows (Re=0), the dimensionless velocity u^* at channel inlet ranging from 0.25 to 1.0, the power-law coefficient *n*=0.5 and the jump number *J*=1, have been shown. As it may be noticed, all unyielded regions decreased with the growth of dimensionless velocity u^*. The plug-flow regions of upstream and downstream channels have strongly decreased when the dimensionless velocity increased from *u**=0.25 (Fig. 4a) to 1.0 (Fig. 4b). In the other unyielded regions, namely the islands above the cylinder at mid distance between cylinder and channel wall, and the polar caps at centerline – according to the nomenclature introduced by Zisis and Mitsoulis (2002), the flow-rate increasing also produced a decrease of these zones – see Fig. 4a, for *u**=0.25, and Fig. 4b, for *u**=1.0. This behavior maybe explained by the shear-rate increasing imposed by the increasing of u^*, which causes shear stresses greater than the yield stress ($\tau > \tau_0$). Another point to be highlighted is the perfect symmetry presented by τ-isobands and horizontal velocity profiles upstream and downstream of the cylinder (see, for instance, Naccache and Barbosa (2007)). This theoretical feature on fluid dynamics of inertialess flows has been well-captured by the multi-field stabilized method employed in the numerical simulations of this article.
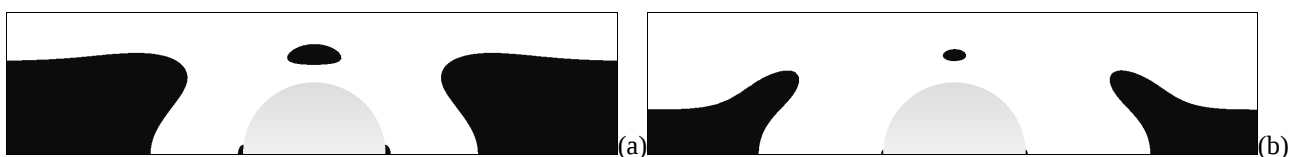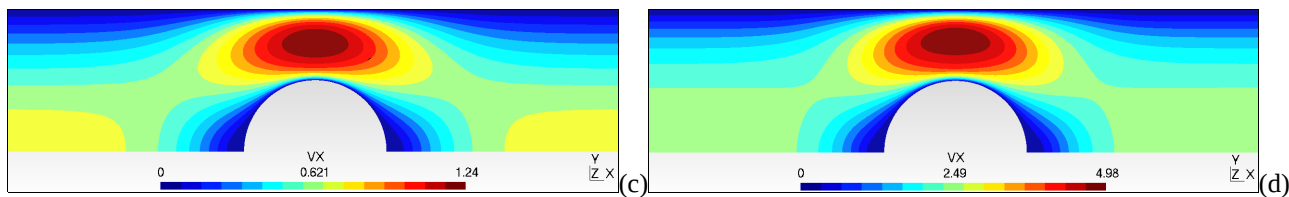
Figure 4. Yield surfaces and axial velocity elevation plots, for Re=0, *n*=0.5 and *J*=1: (a) *u**=0.25; (b) *u**=1.0; (c) *u**=0.25; (d) *u**=1.0.

The influence of inertia on SMD viscoplastic fluid flows was also taken into account in this work and is shown in Fig. 5 and Fig 6. The numerical simulations were performed varying the Reynolds number from 4.0 to 29.05, *n*=0.5 and *J*=1.0. As it may be observed, the fully-developed unyielded zones decreased with the growth of the inertia effects. Besides, the symmetry between these unyielded regions upstream and downstream of the cylinder has disappeared – on the contrary of what was verified on τ-isobands, velocity profiles and pressure contours in the inertialess flows shown in Fig. 3 and 4. The inertia growth has also given rise to asymmetric islands above the equator and polar caps. Even for the lowest value of Reynolds number (Re=4.0, Fig. 6a), it may be noticed the development of a tiny polar cap at the back-flow zone just downstream of the cylinder – a back-flow region subjected to low shear rates. The more the Reynolds number has increased, the more the vortex and the unyielded regions at polar caps have increased too, until the detachment of the unyielded region from the cylinder surface (Fig. 6d). On the opposite way, the islands over the equator - regions subjected to high strain rates – have decreased as Reynolds number increased.
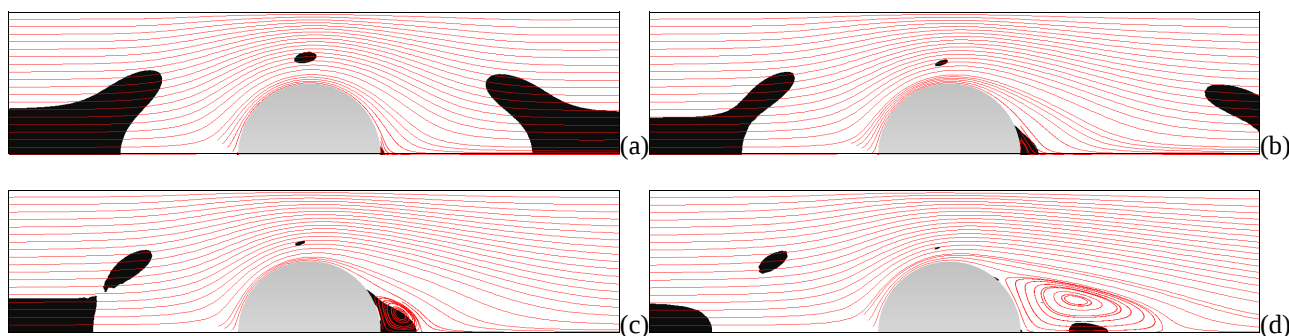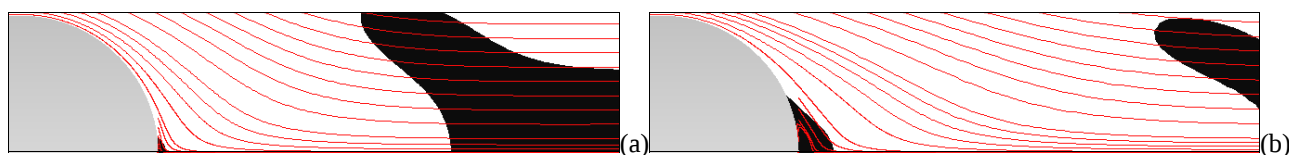

Figure 5. Yield surfaces and flow streamlines, for *n*=0.5 and *J*=1: (a) Re=4.0; (b) Re=11.31; (c) Re=15.81; (d) Re=29.05.

5. FINAL CONCLUSIONS

In this article, finite element approximations for flows of non-linear viscoplastic materials, employing the recently fluid model introduced by Souza Mendes and Dutra (2004), have been carried out. The mechanical model defined by Eq. (1) was composed by continuity and momentum equations coupled with the SMD viscoplastic viscosity function (Eq. (6)). This model has been approximated via a multi-field stabilized method, defined by Eq. (10)-(13), that used equal-order bi-linear Lagrangian interpolations for extra-stress, velocity and pressure fields – a combination of interpolations *a priori* not satisfying the inf-sup compatibility conditions involving the finite element sub-spaces for velocity and pressure and for extra-stress and velocity.

The numerical simulations of SMD viscoplastic fluids around a circular cylinder, confined inside a planar channel, have led to some conclusions. First, for creeping flows, it may be observed that the increasing either of the dimensionless inlet velocity or the jump number have decreased the size of material unyielded zones. After, for inertia flows, the more the Reynolds number increased, the more the unyielded moving zones decreased and the vortex length just downstream the cylinder increased. In addition, the symmetry, the stability and smoothness of the numerical results have confirmed the fine features of the multi-field stabilized formulation employed in this work.
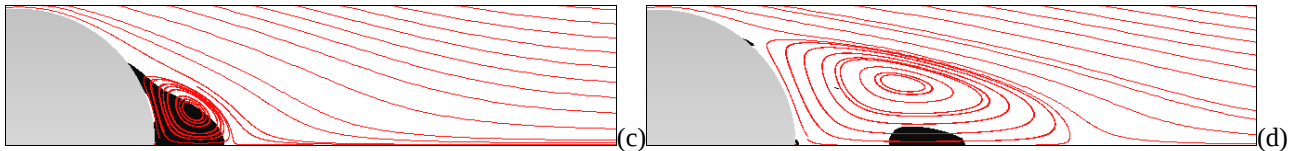
Figure 6. A detail of yield surfaces and flow streamlines, for *n*=0.5 and *J*=1: (a) Re=4.0; (b) Re=11.31; (c) Re=15.81; (d) Re=29.05.

6. ACKNOWLEDGEMENTS

7. REFERENCES

Astarita, G. and Marrucci. G., 1974, "Principles of Non-Newtonian Fluid Mechanics". Vol. 1, John Wiley & Sons, U.S.A.

Barnes, 1999., "The yield stress – a review or 'παντα ρει' - everything flows?", J. Non-Newtonian Fluid Mech, Vol. 81, pp.133-178.

Behr, M., Franca, L.P. and Tezduyar, T.E., 1993, "Stabilized Finite Element Methods for the Velocity-Pressure-Stress Formulation of Incompressible Flows", Comput. Methods Appl. Mech. Engrg., Vol. 104, pp. 31-48.

Bird, R.B., Armstrong, R. C. and Hassager, O., 1987, "Dynamics of Polymeric Liquids". Vol. 1, John Wiley & Sons, U.S.A.

Ciarlet, P.G., 1978, "The Finite Element Method for Elliptic Problems". North Holland, Amsterdam.

Franca, L.P., and Frey, S., 1992, "Stabilized Finite Element Methods: II. The Incompressible Navier-Stokes Equations", Comput. Methods Appl. Mech. Eng., Vol. 99, pp. 209-233.

Hughes, T.J.R., Franca, L.P., Balestra, M., 1986, "A new finite element formulation for computational fluid dynamics: V. Circumventing the Babuška-Brezzi condition: A stable Petrov-Galerkin formulation of the Stokes problem accomodating equal-order interpolations", Comput. Methods Appl. Mech. Eng., Vol. 59, pp. 85-99.

Naccache, M.F. and Barbosa, R. S. , 2007, "Creeping flow of viscoplastic materials through a planar expansion followed by a contraction", Mechanics Research Communications, Vol. 34 , pp. 423-431.

Souza Mendes, P.R., and Dutra, E.S.S., 2004, "Viscosity Function for Yield-Stress Liquids", Applied Rheology, Vol. 14, pp. 296-302.

Souza Mendes, P. R., Naccache, M. F., Varges, P. R., and Marchesini, F. H., 2007,"Flow of viscoplastic liquids through axisymmetric expansions-contractions", J. Non-Newt. Fluid Mech., Vol. 142, pp. 207-217.

Zisis and Mitsoulis, 2002, "Viscoplastic flow around a cylinder kept between parallel plates", J. Non-Newtonian Fluid Mech, Vol. 105, pp.1-20.

8. RESPONSIBILITY NOTICE